Supporting Information

Hexylresorcinol calix[4]arene assisted synthesis of ZnO-Au micro-nano materials with enhanced photodegradation performance to degrade harmful organic compounds

Yufeng Yao, [a,b] Jiayi Yuan, [a] Ming Shen*[b] and Bin Du [b,c]

[a] Center of Analysis and Testing, School of Chemistry & Environmental Engineering, Yancheng Teachers University, Yancheng, Jiangsu 224007, PR China

[b] School of Chemistry and Chemical Engineering, Yangzhou University, Yangzhou, Jiangsu 225002, China, Yangzhou University, Yangzhou, Jiangsu 225002, PR China

[c] College of Chemical Engineering, Yangzhou Polytechnic Institute, Yangzhou, Jiangsu, 225127, China

*Corresponding author.

E-mail address: shenming@yzu.edu.cn (M. Shen).

The morphology of ZnO and ZnO-Au micro-nano materials was measured by FE-SEM. When without the addition of $HAuCl_4$, the flower ZnO with diameter of 2 μm is obtained, as shown in Fig. S1(a). When a small amount of $HAuCl_4$ (0.1030 mL of 9.712×10^{-3} mol/L $HAuCl_4$) is added, the obtained sample is lavender, the flake structure on the flower ball is reduced, and the obtained flower ball is incomplete (Fig. S1(b)). After increasing the amount of Au, the colour of the obtained sample is darkened, the ball-flower become incomplete and lamellae decrease (Figs. S1(c) and (d)). When the amount of Au is 2.5 mol% (S4), the ball-flower thoroughly disappears and only sheet structure can be obtained, as shown in Fig. S1(e). Therefore, it can be seen that the amount of $HAuCl_4$ have a great influence on the morphology of particles. Maybe this is due to the fact that under alkaline conditions, $HAuCl_4$ can be rapidly reduced by the phenolic hydroxyl in HRCA to metallic Au nanoparticles, which adhere to the surface of ZnO, thus hindering the deposition of newly formed ZnO-Au nanoflakes at these locations. The newly formed flake ZnO-Au micro-nano materials can't aggregate and only exist as flake in the reaction system.

To further confirm the influence of Au on the morphology of ZnO, TEM characterization was carried out. As Fig. S1(g) shown, pure ZnO is consisted of 2 μm flower ball. When there is a small amount of Au, the size of particles decreases to 1 μm and it can be seen that there is a superposition of pieces, but the thickness decreases obviously (Fig. S1(h)). With the increase of Au content (such as 2.5 mol% and 5 mol%), the flower ball gradually disappears, and a single layer of ZnO flake appears, and there are black spots on the flake, these could be Au nanoparticles adhering onto the ZnO flake (Figs. S1(k) and (l)). It is obvious that these are consistent with the previous FE-SEM results.

To obtain detailed information about the structure of the fabricated ZnO-Au micro-nano materials, HRTEM and EDS mapping of S3 were further measured. The measured *d* spacings of S3 are 0.26 and 0.23 nm (Fig. S1(m)), which are consistent with the crystal plane (002) of ZnO and crystal plane (111) of metallic Au, respectively.[1,2] Furthermore, the Zn element and O element are found to be evenly dispersed on the selected area from the EDS images of S3 (Fig. S1(n)). However, Au nanoparticles are scattered on the surface of the sample. The HRTEM and EDS images evidently suggest that the Au nanoparticles are distributed on the surface of ZnO slices in a granular form.

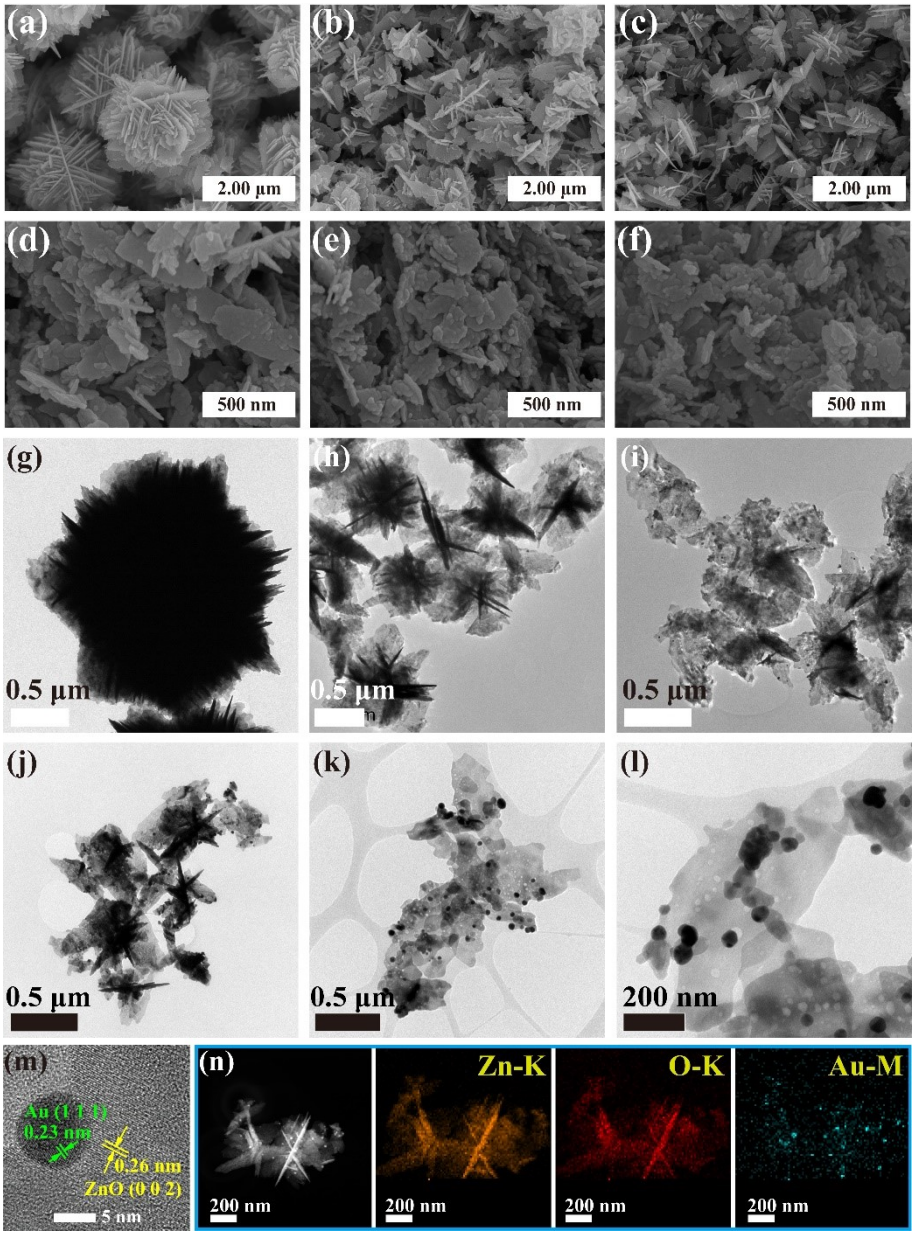

Fig. S1. FE-SEM images: (a) S, (b) S1, (c) S2, (d) S3, (e) S4, and (f) S5. TEM pictures: (g) S, (h) S1, (i) S2, (j) S3, (k) S4, and (l) S5. (m) HRTEM of S3. (n) EDS mapping imagines of S3.

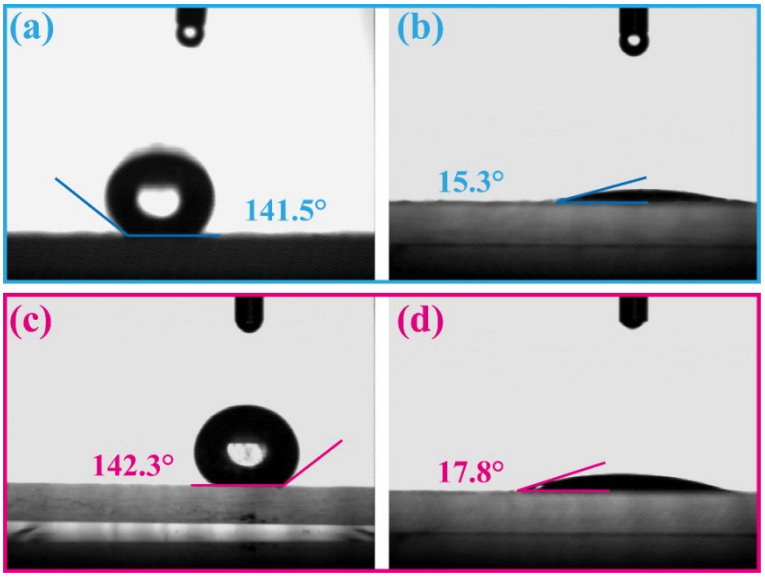

Fig. S2. Contact angles of ZnO samples ((a) and (b)) and ZnO-Au samples ((c) and (d)) with theoretical molar relative content of Au of 1.0 mol%: (a) and (c) before calcination，(b) and (d) after calcination.

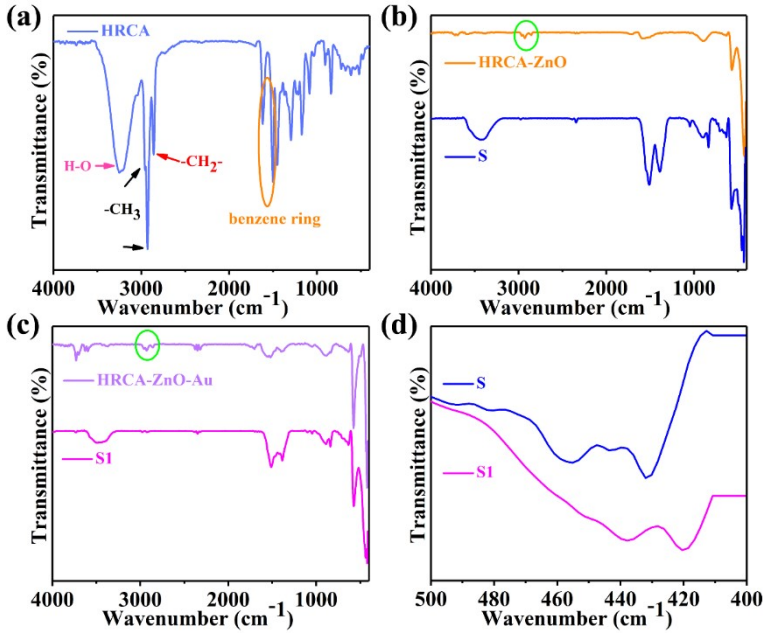

Fig. S3. FT-IR spectra of the prepared samples: (a) HRCA, (b) HRCA-ZnO and S, (c) HRCA-ZnO-Au and S1, (d) 500~400 cm^{-1}.

Fig. S4(a) shows the photoluminescence (PL) spectra of ZnO-Au. There are two emission bands: one is centred at 382 nm belonged to the weak UV emission band, which is caused by the near-band-edge of ZnO;[3] and another is a broad and strong yellow emission

band at approximately 600 nm which is commonly originated from defect states of oxygen vacancies.[4] And the intensity of PL spectrum significantly reduces with the molar ratio of Au increase, which indicates that the sample with higher Au content exhibit better electron-hole separation effect.[3] The improvement of electron-hole pairs separation efficiency is conducive to the production of more active substances.[5]

UV-vis DRS were tested to determine the optical properties of different samples and the surface plasmon resonance of Au nanoparticles in ZnO-Au micro-nano materials. As illustrated in Fig. S4(b), pure ZnO only displays a significant absorption in the UV range with absorption edge about 370 nm, which corresponds to the wide band gap of ZnO.[6] When only loaded with 0.1 mol% Au, the absorption spectrum of S1 varies greatly, namely, except for the ultraviolet signal at 370 nm, a new wide peak appears at visible fraction from 450 to 800 nm, which corresponds to the surface plasma resonance absorption of Au.[7] And with the Au content increase, this visible absorption increases, because of the surface plasmon resonance signal of Au nanoparticles enhancing.[8] The UV-vis DRS results are also unanimous with the phenomenon that the colour of the samples changes from white to light purple and deep purple. By the linear extension method, the valence band maximum (VBM) value of ZnO is determined to be 2.51 eV (Fig. S4(d)),[9] while the conduction band minimum (CBM) value is calculated as −0.71 eV based on E_g and VBM.[10]

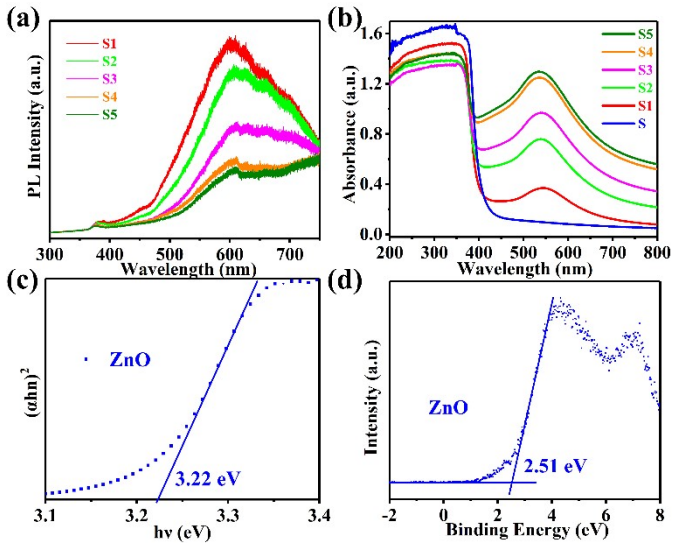

Fig. S4. (a) PL spectra of ZnO-Au micro-nano materials. (b) UV-vis DRS of the samples. (c) Band gap of pure ZnO. (d) XPS valence band spectra of ZnO.

Fig. S5 shows the UV-vis spectra of degraded solution with S5 as the photocatalyst, under simulated sunlight irradiation. The characteristic absorption peaks of RhB or levofloxacin hydrochloride were close to 0 after 30 min or 48 min respectively.

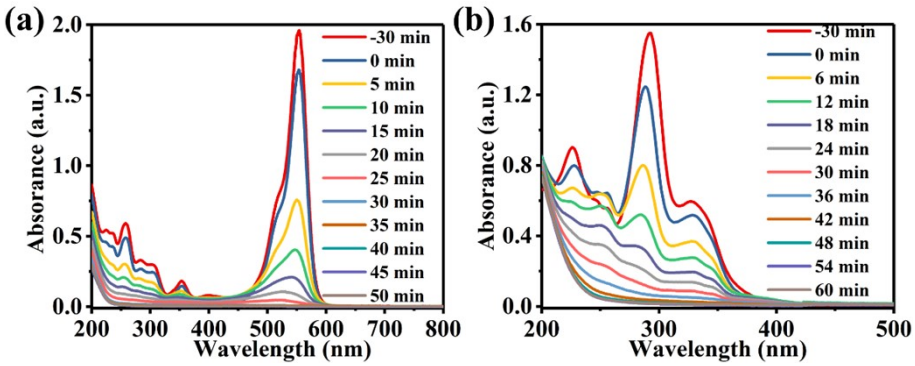

Fig. S5. The UV-vis spectra of the degraded solutions at different times when using S5 as photocatalyst: (a) RhB and (b) levofloxacin hydrochloride.

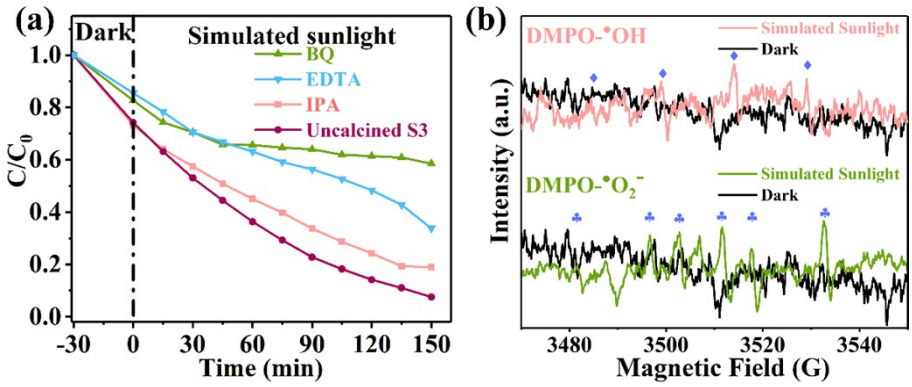

Fig. S6. (a) The indirect capturing free radicals of uncalcined S3. (b) EPR spectra of uncalcined S3.

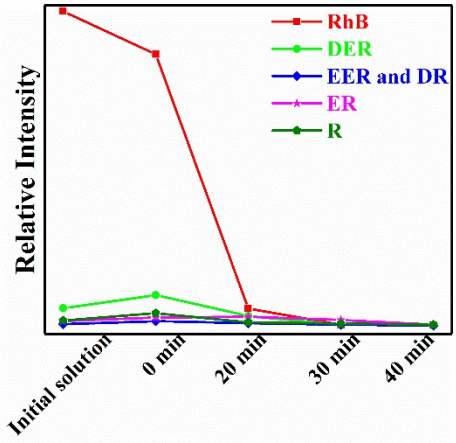

Fig. S7. The relative content of each intermediate.

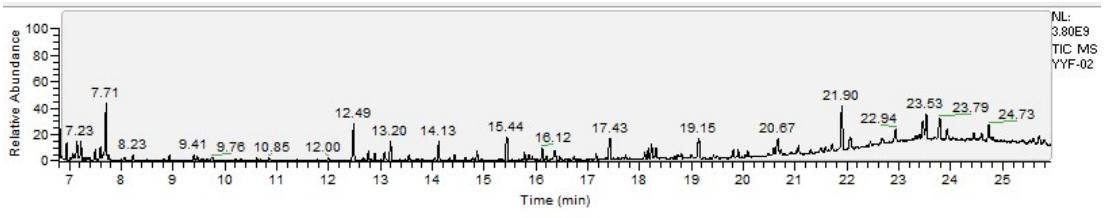

Fig. S8. Gas chromatogram of RhB degradation products.

Table S1. The possible small organic molecules in RhB degradation products by GC-MS.

product	retention time min	molar mass	formula	product name
1	7.71	135	$C_9H_{13}N$	2-phenylalanine
2	7.71	177	$C_{10}H_{11}NO_2$	Phthalic acid amide
3	9.39	94	C_6H_6O	phenol
4	7.71	88	$C_4H_{12}N_2$	1,4-butanediamine

5	7.71	45	C_2H_7N	ethylamine
6	7.71	75	$C_2H_5NO_2$	1-aminoacetic acid
7	8.23	62	$C_2H_6O_2$	glycol
8	8.23	90	$C_2H_2O_4$	oxalic acid
9	8.23	76	$C_2H_4O_3$	1-ol-acetic acid
10	12.49	122	$C_7H_6O_2$	benzoic acid
11	14.12	138	$C_7H_6O_3$	4-phenol benzoic acid
12	15.43	154	$C_7H_6O_4$	1,5-bisphenol benzoic acid
13	15.43	152	$C_8H_8O_3$	2-phenol-3-methylbenzoic acid

References

1 Y. Cheng, W. Wang, L. Yao, J. Wang, Y. Liang and J. Fu, Insights into charge transfer and solar light photocatalytic activity induced by the synergistic effect of defect state and plasmon in Au nanoparticle-decorated hierarchical 3D porous ZnO microspheres, *Appl. Surf. Sci.*, **2019**, 494, 959–968.

2 Y. F. Cheng, W. Jiao, Q. Li, Y. Zhang, S. Li, D. Li and R. Che, Two hybrid Au-ZnO aggregates with different hierarchical structures: A comparable study in photocatalysis, *J. Colloid Interface Sci.*, **2018,** 509, 58–67.

3 S. J. Lee, H. J. Jung, R. Koutavarapu, S. H. Lee, M. Arumugam, J. H. Kim and M. Y. Choi, ZnO supported Au/Pd bimetallic nanocomposites for plasmon improved photocatalytic activity for methylene blue degradation under visible light irradiation, *Appl. Surf. Sci.*, **2019**, 496, 143665.

4 T. Liu, W. Chen, Y. Hua and X. Liu, Au/ZnO nanoarchitectures with Au as both supporter and antenna of visible-light, *Appl. Surf. Sci.*, **2017**, 392, 616–623.

5 J. Q. Chang, Y. Zhong, C. H. Hu, J. L. Luo and P. G. Wang, Study on highly efficient BiOCl/ZnO p-n heterojunction: Synthesis, characterization and visible-light-excited photocatalytic activity, *J. Mol. Struct.*, **2019**, 1183, 209–216.

6 Y. S. Xie, N. Zhang, Z. R. Tang, M. Anpo and Y. J. Xu, Tip-grafted Ag-ZnO nanorod arrays decorated with Au clusters for enhanced photocatalysis, *Catal. Today.*, **2020**, 340, 121–127.

7 W. Zhang, W. Wang, H. Shi, Y. Liang, J. Fu and M. Zhu, Surface plasmon-driven photoelectrochemical water splitting of aligned ZnO nanorod arrays decorated with loading-controllable Au nanoparticles, *Sol. Energy Mater. Sol. Cells*, **2018**, 180, 25–33.

8 V. Vaiano, C. A. Jaramillo-Paez, M. Matarangolo, J. A. Navío and M. del Carmen Hidalgo, UV and visible-light driven photocatalytic removal of caffeine using ZnO modified with different noble metals (Pt, Ag and Au), *Mater. Res. Bull.*, **2019**, 112, 251–260.

9 N. Li, J. Zhang, Y. Tian, J. Zhao, J. Zhang and W. Zuo, Precisely controlled fabrication of magnetic 3D γ-Fe_2O_3@ZnO core-shell photocatalyst with enhanced activity: Ciprofloxacin degradation and mechanism insight, *Chem. Eng., J.*, **2017**, 308, 377–385.

10 N. Li, Y. Tian, J. Zhang, Z. Sun, J. Zhao, J. Zhang and W. Zuo, Precisely-controlled modification of PVDF membranes with 3D TiO_2/ZnO nanolayer: enhanced anti-fouling performance by changing hydrophilicity and photocatalysis under visible light irradiation, *J. Memb. Sci.*, **2017**, 528, 359–368.